J Mater Sci (2009) 44:351–357
DOI 10.1007/s10853-008-3105-0

The effects of strain rate, density, and temperature on the mechanical properties of polymethylene diisocyanate (PMDI)-based rigid polyurethane foams during compression

Bo Song · Wei-Yang Lu · Chul Jin Syn · Weinong Chen

Received: 6 August 2008 / Accepted: 4 November 2008 / Published online: 26 December 2008

Abstract Compressive experiments on three types of rigid polyurethane foams were conducted by employing modified split Hopkinson pressure bars (SHPBs). The foam materials, which were based on polymethylene diisocyanate (PMDI), varied only in density (0.31×10^3, 0.41×10^3, and 0.55×10^3 kg/m^3) and were compressed at strain rates as high as 3×10^3 s^{-1}. Dynamic experiments were also performed on these three foam materials at temperatures ranging from 219 to 347 K, while maintaining a fixed high strain rate of $\sim 3 \times 10^3$ s^{-1}. In addition, an MTS materials testing frame was used to characterize the low-strain-rate compressive response of these three foam materials at room temperature (295 K). Our study determined the effects of density, strain rate, and temperature on the compressive response of the foam materials, resulting in a compressive stress–strain curve for each material.

Introduction

Polymeric foam materials are widely used as encapsulants to protect critical electronic and magnetic assemblies from mechanical damage in the event of vibration or impact loading [1]. Like epoxy syntactic foam materials [2], toluene diisocyanate (TDI) and polymethylene diisocyanate (PMDI) polyurethane foams provide excellent survivability for encapsulated devices that are subject to vibration or impact loading [3]. Compared with TDI foam, PMDI foam is easier to work with and is more environmental friendly. Because of these advantages, PMDI foam has replaced TDI foam as a structural component in many applications. For example, PMDI foam has been used in a structure to mitigate the mechanical shock—created upon impact—to the internal components [3]. Such applications benefit from PMDI foam materials, which are lightweight and exhibit high-strength mechanical properties. However, the mechanical properties of PMDI foam under a variety of loading and environmental conditions—especially extreme conditions—have not been fully understood.

In both the military and transportation arenas, a primary concern regarding potential applications of PMDI foam is the weight of the integrated components. Optimizing the structural efficiency of such applications requires first determining the appropriate density of the packaging foam material. In addition, to effective protection of internal devices encapsulated by a foam material, the foam's mechanical parameters, such as its elastic modulus and yield strength, must be known. The mechanical response of foam materials depends on the density of the foam, as well as external conditions such as the rate of loading (or strain rate) and environmental temperature [4, 5]. The effect of strain rate takes the form of significant changes in the mechanical response of engineering materials when subjected to the strain rates incurred in impact events. These strain rates are typically several orders higher than those of quasi-static events. A universal materials testing frame (e.g., an MTS) is generally unable to perform high-strain-rate testing. Thus, specific testing techniques are required for mechanical experiments at high strain rates.

By using a split Hopkinson pressure bar (SHPB), Bateman et al. [3] investigated the high-rate compressive

B. Song (✉) · W.-Y. Lu
Sandia National Laboratories, Livermore, CA 94551, USA
e-mail: bsong@sandia.gov

C. J. Syn · W. Chen
Schools of AAE & MSE, Purdue University, 701 W. Stadium Avenue, West Lafayette, IN 47907, USA

response of PMDI foam materials at two different densities (0.16×10^3 and 0.32×10^3 kg/m^3). The researchers also studied the effects of confining pressure and specimen length on the dynamic response of materials. However, in this pioneering study, the deformation of foam specimens was relatively small. In addition, the validity of the study's testing conditions should be carefully considered since more recent research [6] indicates that SHPBs must be modified when used to test foam materials.

In the experimental series described in this paper, we employed an appropriately modified SHPB to perform compression experiments on three types of PMDI foam materials at high strain rates. These foam materials differed only in foam density. Our experimental data also include the low-strain-rate results we obtained by using an MTS materials testing frame. Consequently, we are able to present experimental results of strain-rate effects over a wide range.

To investigate the high-rate compressive response of our three foam materials at various temperatures, we used a heating/cooling device in conjunction with the modified SHPB. Our experimental results enabled us to produce compressive stress–strain curves and determine the effects of density, strain rate, and temperature on the foam material's yield strength. In addition to developing strain-rate-, density-, and temperature-dependent material models, our investigation of both strain-rate and temperature effects is potentially attractive for understanding the temperature–time (or strain-rate) superposition principle for foam materials of different densities [7, 8].

Materials and specimens

The PMDI foam material was prepared at the Kansas City Plant, Kansas City, MO, to meet three target densities: 0.32×10^3, 0.48×10^3, and 0.64×10^3 kg/m^3. The foam densities were produced by controlling the volume fraction of the cells. The actual densities of the foam specimens in this study were slightly different from the proposed values. Moreover, the density of the foam specimens varied slightly within each target density; this slight variance was attributed to the foam materials' unique manufacturing process. Figure 1 shows the variation in specimen density for these three proposed densities. The solid lines indicate the average foam densities (0.31×10^3, 0.41×10^3, and 0.55×10^3 kg/m^3), which are slightly less than the proposed values (dashed lines). Figure 2a, b, and c shows the respective microstructures of the foam materials. According to these scanning electronic microscopy images, each of the PMDI foam materials has a closed-cell structure. The cell diameter varies from 100 to 200 μm for all three densities, which is consistent with the results obtained by Jin et al. [9].

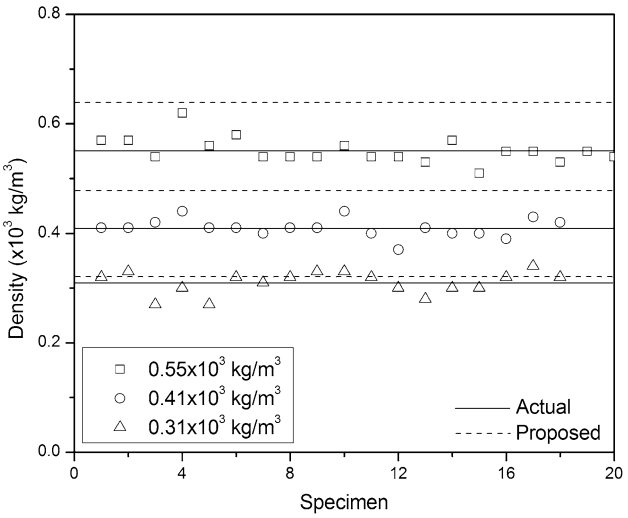

Fig. 1 Density scattering plot showing the variation in specimen density for the three proposed foam-material densities

One fundamental requirement for a valid SHPB experiment is dynamic stress equilibrium. In other words, to obtain a valid stress–strain response for a material, the specimen must be in a uniform stress/strain state. For high-strain-rate testing, this requirement is even more critical, especially when the tested material is soft—such as foam materials—because the stress in the specimen typically cannot be equilibrated within a very short loading duration. Recent research findings recommend using thin specimens and proper pulse-shaping techniques to facilitate dynamic stress equilibrium in SHPB experiments [6, 10].

Specimen thickness may not be as critical for quasi-static experiments as for dynamic experiments. However, a specimen that is too thick may result in a nonuniform deformation [11]. Bateman et al. [3] found that specimen length influences the yield strength of the foam material. In our study, the foam specimens in both the dynamic and quasi-static experiments had the same dimensions: 4.3 mm thick and measuring 13.0 mm in diameter. Over the 4.3-mm thickness, 25–50 cells can be lined up, which is sufficient for material characterization. This consistency in specimen dimensions ensured that any effects resulted solely from strain-rate variations.

Experiments

Dynamic experiments were conducted with a modified SHPB at Purdue University. The required modifications when using an SHPB for testing foam materials have recently been reviewed and documented [6]. Figure 3 shows a schematic of the modified SHPB that we employed for foam testing. The bars used in this study were made of 7075-T651 aluminum alloy and had a common diameter of

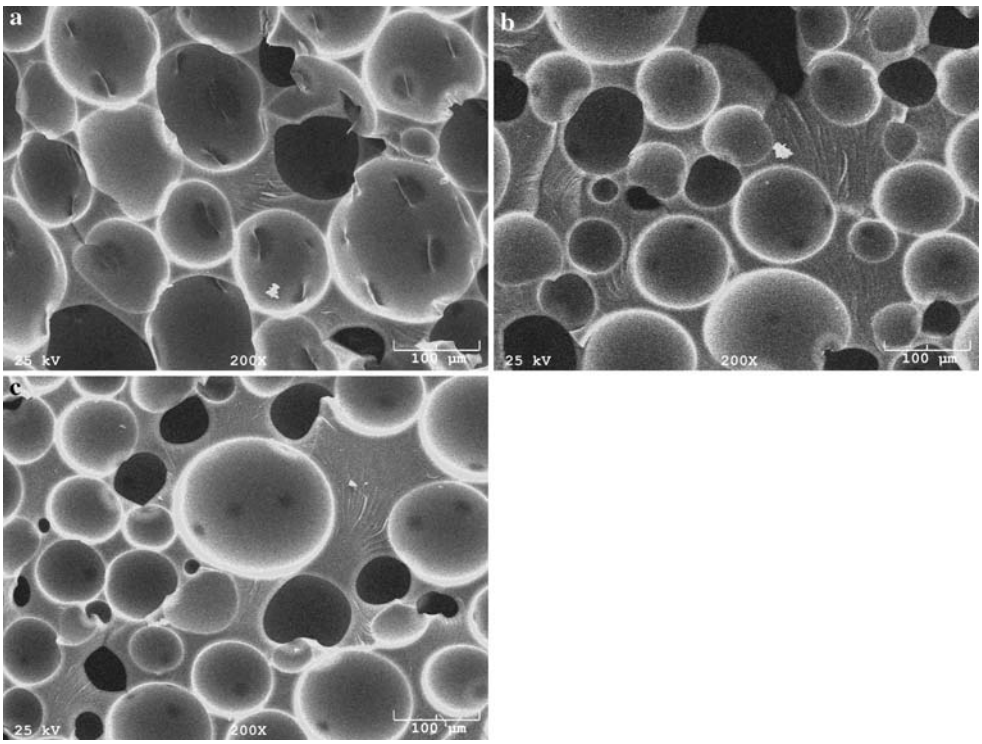

Fig. 2 Scanning electron microscopy images of cell structures in our experimental foam materials, which varied only in density: **a** 0.31 × 10^3 kg/m^3, **b** 0.41 × 10^3 kg/m^3, and **c** 0.55 × 10^3 kg/m^3

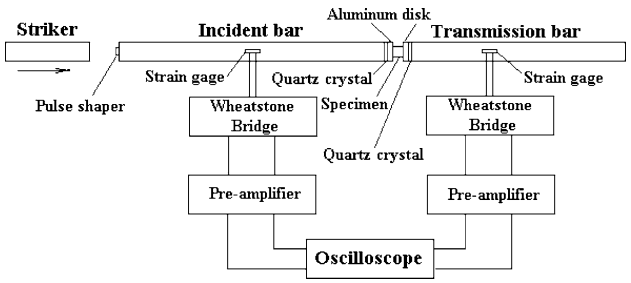

Fig. 3 A schematic of the experimental SHPB, as modified for testing foam materials

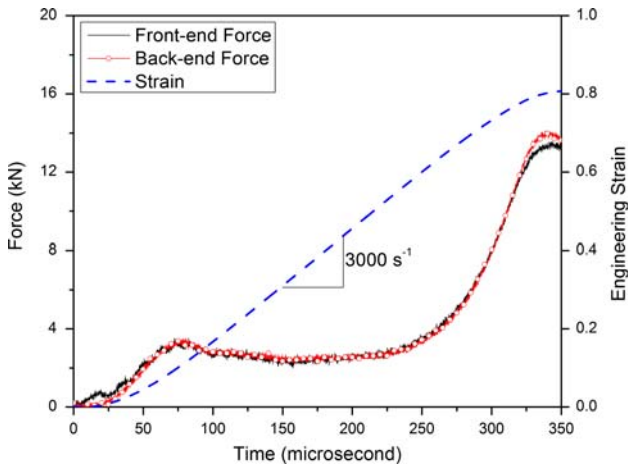

Fig. 4 Force equilibrium and strain-rate history in an SHPB experiment with a 0.31 × 10^3 kg/m^3 foam specimen

19.05 mm. As shown in Fig. 3, the SHPB was modified by attaching a pulse shaper to the impact end of the incident bar and by adding quartz-crystal force transducers to the specimen ends of the pressure bars. The pulse shaper, which shapes the incident-loading pulse, ensures the specimen's deformation at a constant strain rate under a dynamic stress/force equilibrium. The quartz-crystal force transducers directly monitor the process of dynamic force equilibrium in the foam specimen, a phenomenon that cannot be monitored through conventional methods [6]. The impact of the striker on the pulse-shaper end of the incident bar generates a compressive stress wave that propagates through the incident bar until the wave arrives at the specimen. At the bar/specimen interface, part of the stress wave is reflected back to the incident bar, and the remainder of the wave transmits into the transmission bar while the specimen is compressed. The strain gages on both the incident and transmission bars record the incident, reflected, and transmitted pulses. These records are then used to calculate the mechanical parameters (e.g., stress, strain, and strain rates) of the tested specimen.

Figure 4 shows a typical strain history and force equilibrium process, as observed in a 0.31 × 10^3 kg/m^3 foam

specimen. In this figure, the forces at both ends of the specimen nearly overlap, which shows that the force in the specimen has equilibrated. Furthermore, the slope of the nearly linear strain history demonstrates that the foam specimen was compressed at a constant strain rate of 3×10^3 s^{-1}. After the force is equilibrated in the foam specimen, the stress–strain curve at this constant strain rate can be calculated by using conventional methods [12].

By varying the striking speed of the striker and the dimensions of the pulse shaper, the foam specimens were compressed at different constant strain rates to investigate strain-rate effects. The standard SHPB is limited by loading duration, so it cannot compress specimens to large deformations at relatively lower strain rates [13, 14]. Thus, to conduct dynamic experiments at a lower strain rate of $\sim 4 \times 10^2$ s^{-1} in our study, we employed a long SHPB (LSHPB) [15]. The LSHPB technique can be used to conduct experiments on foam materials at strain rates on the order of 10^1 s^{-1}, which is very close to the upper bound of strain rates in MTS experiments [14, 15]. In our study, MTS experiments were also conducted at strain rates on the order of 10^{-2} and 10^0 s^{-1} under the control of displacement. Consequently, the compressive stress–strain curves for all three foam materials were obtained in the strain-rate range of 10^{-2} to 10^3 s^{-1}.

To study the effects of temperature on the compression of PMDI foam materials, we also conducted dynamic compression experiments at various set temperatures (219, 261, 323, and 347 K), as well as at room temperature (295 K). These experiments had a fixed dynamic strain rate of 3×10^3 s^{-1}. A heating/cooling chamber was used to control temperature in the experiment [5], and the temperature inside the chamber was monitored with a thermocouple that was embedded very close to the specimen. Higher temperatures were automatically maintained by a WATLOW® controller (96A0-DAAA-00RG), which controlled several interior ceramic heating elements. In contrast, a low-temperature environment for the foam specimens was created by pouring liquid nitrogen into a circulated brass tube inside the chamber. The cold environmental temperature in the chamber was then maintained by manually adjusting the flow rate of liquid nitrogen in the brass tube. The temperature was the only variable in this set of experiments. Other variables, such as density and strain rate, were maintained to be nearly identical.

As shown in Fig. 1, foam specimens in each of the three density categories exhibited a slight variation in density. To minimize the effect of density variation, we repeated four experiments under identical testing conditions. We then used the mean curve from the four repeated experiments to represent the overall compressive response of the foam material.

Experimental results

The compressive stress–strain curves of the three foam materials (at densities of 0.31×10^3, 0.41×10^3, and 0.55×10^3 kg/m^3) at various strain rates are shown in Fig. 5a, b, and c, respectively. The data for these stress–strain curves were obtained at room temperature (295 K). The stress–strain curves for these three foam materials shared a common characteristic: an initial linearly elastic response followed by a collapse process of cell structures. After all of the cell structures collapsed, the foams began to condense, as shown by the increasing stress amplitude in the stress–strain response [1]. However, this characteristic varied slightly at different strain rates for each foam material; this variation was especially apparent in the cell-structure collapse process. At quasi-static strain rates, the stress–strain curves exhibited a long plateau, or slow work-hardening behavior, after yielding. This plateau may indicate the plastic buckling of the cell structures under quasi-static loading. However, at dynamic strain rates, the stress dropped from the yield strength, causing the stress–strain curves to assume an "N" shape. This drop in stress was caused by the sudden collapse of cell structures under high-strain-rate loading. Thus, the strain rate influenced the deformation/damage mechanism in the foam material's cell structures.

Strain rate was also found to influence yield strength. The yield strength for all three foam materials increased with strain rate. Figure 6 shows the detailed strain-rate effect on yield strength for these three foam materials. The yield strength of the three foam materials linearly increases with the logarithm of strain rate, as shown in Eq. 1:

$$\sigma_y = A + B \log(\dot{\varepsilon}/\dot{\varepsilon}_0) \quad (1)$$

where A and B are constants with values listed in Table 1, and $\dot{\varepsilon}_0$ is the reference strain rate, $\dot{\varepsilon}_0 = 1 \times 10^{-2}$ s^{-1}. The constant B represents the yield strength's sensitivity to strain rate. In Fig. 6, the slope of each solid line represents the strain-rate sensitivity for each foam-material density. The parallel lines in Fig. 6 imply that the strain-rate sensitivity for the 0.31×10^3 kg/m^3 foam material is very similar to that of the 0.41×10^3 kg/m^3 foam. Both are lower than that of the 0.55×10^3 kg/m^3 foam.

As shown in Fig. 5a, b, and c, at similar high strain rates, the "N" shape in the stress–strain curves was more severe for higher-density foam materials. For example, at a strain rate of 1,500 s^{-1}, the stress for the 0.55×10^3 kg/m^3 foam material dropped by $\sim$55% from the yield strength while the stress for the 0.41×10^3 kg/m^3 foam material decreased by $\sim$32% from the yield strength. However, the decrease was only 20% for the 0.31×10^3 kg/m^3 foam. These phenomena imply that the cell structures in foam

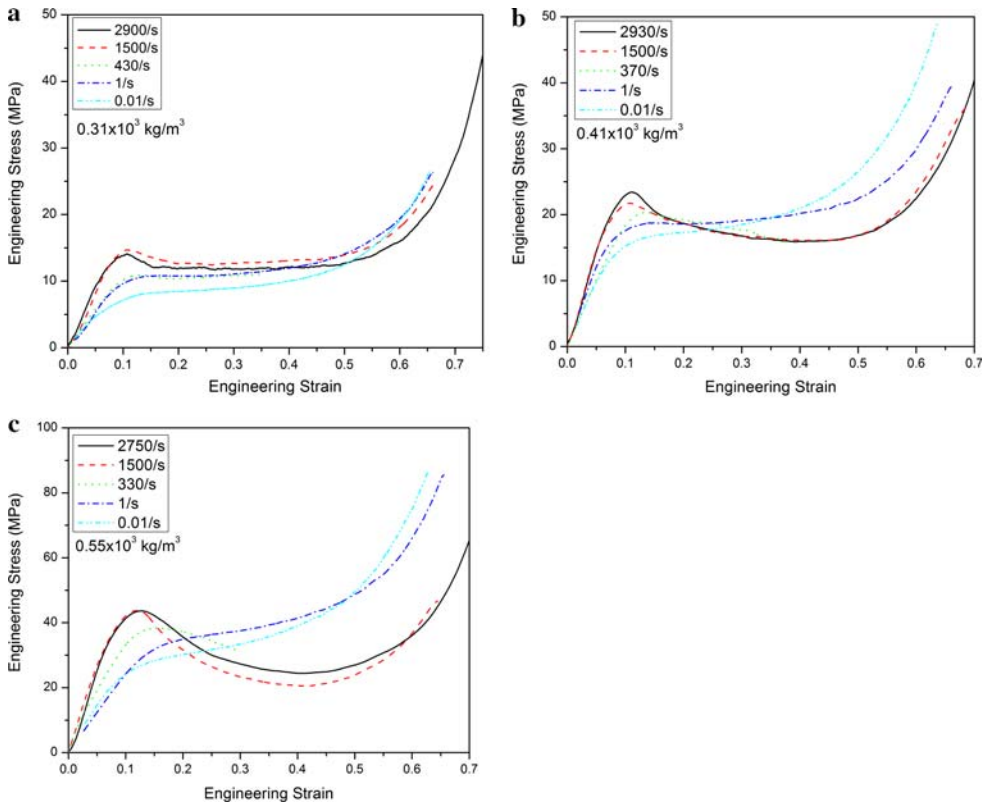

Fig. 5 Compressive stress–strain curves at various strain rates for our three foam-material densities: **a** 0.31 × 10^3 kg/m^3, **b** 0.41 × 10^3 kg/m^3, and **c** 0.55 × 10^3 kg/m^3

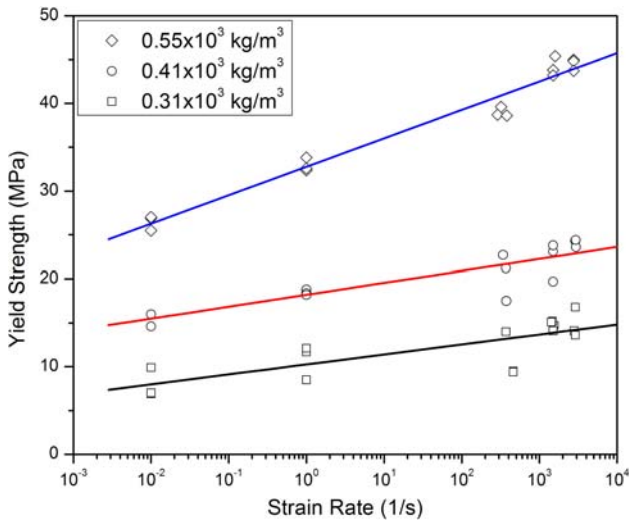

Fig. 6 Strain-rate sensitivities of the foam materials at different densities

Table 1 Material constants in Eqs. 1 and 3

Density (×10^3 kg/m^3)	A (MPa)	B (MPa)	C (MPa)	D (MPa)
0.31	7.98	1.14	−14.75	28.90
0.41	15.48	1.36	−12.39	24.92
0.55	26.27	3.25	−35.40	76.74

specimens with higher densities collapsed more severely under impact loading.

Density also significantly influenced yield strength. In Eq. 2, we use σ_{y20}, the yield strength of the 0.31 × 10^3 kg/m^3 foam, as the reference for determining the relative increase of yield strength, β, for the 0.41 × 10^3 and 0.55 × 10^3 kg/m^3 foam materials:

$$\beta = \frac{(\sigma_y - \sigma_{y20})}{\sigma_{y20}} = \frac{\Delta\sigma_y}{\sigma_{y20}} \quad (2)$$

The β parameter indicates the effect of density on the yield strength for PMDI foam materials. As shown in Fig. 7, the value of β depends on both density and strain rate. Compared to the 0.31 × 10^3 kg/m^3 foam, the yield strengths increased by approximately 60–90% and 205–225%, depending on the strain rate, for the 0.41 × 10^3 and 0.55 × 10^3 kg/m^3 foam materials, respectively. The value of β also linearly decreased as the logarithm of strain rate increased.

Figure 8a, b, and c shows the compressive stress–strain curves of the three foam materials at various temperatures. The strain rate in all of these stress–strain curves was controlled to 3 × 10^3 s^{-1} ±5%. For foam materials with a certain density, temperature influenced not only the material's yield strength but also the shape of the stress–strain curve. This temperature effect was especially strong in the 0.55 × 10^3 kg/m^3 foam material. As shown in Fig. 8,

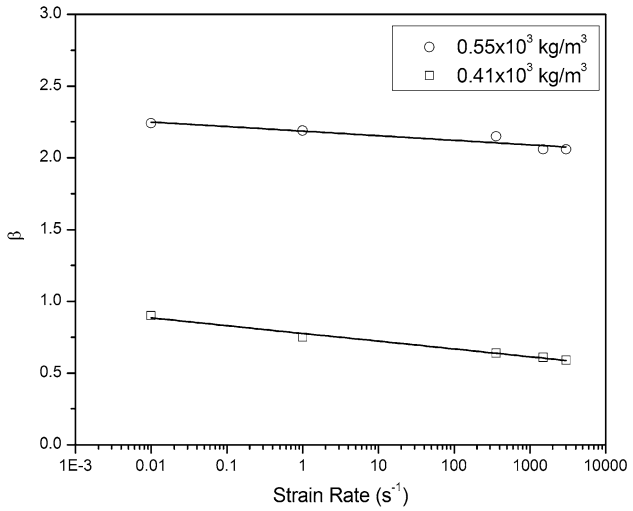

Fig. 7 The effect of density on the PMDI foam material's yield strength at various strain rates

almost all of the stress–strain curves exhibited an "N" shape. The curve obtained at the temperature of 347 K was the one exception: this stress–strain curve showed a long plateau, which was very similar to the curves obtained at low strain rates (Fig. 5).

The variation in stress–strain curves can be attributed to different deformation and collapse mechanisms at different temperatures. As a sort of polymer, the foam matrix is very sensitive to temperature. The material exhibits more brittle behavior at lower temperatures and is more ductile when the temperature is higher. The material's brittle feature at low temperatures causes the sudden collapse of the cell structures, which then results in a decrease in load-bearing capability. In contrast, the material's high ductility at high temperatures causes cell structures to deform via plastic buckling rather than sudden collapse. Even under impact loading, the 0.55×10^3 kg/m^3 foam specimen still had a consistent load-bearing capability at high temperatures, showing a plateau in the stress–strain curve.

For the foam materials with densities of 0.31×10^3 and 0.41×10^3 kg/m^3, the compressive stress–strain curves at different temperatures had very similar characteristics although the elastic behavior and yield strength of both materials were sensitive to temperature. Yield strength increased with decreasing temperature for all three foam materials. However, the sensitivity of yield strength to the temperature depended on the density of the foam material. Similar to strain-rate sensitivity, temperature sensitivity, σ_Y is described by the following linear relationship,

$$\sigma_Y = C \cdot \frac{T}{T_0} + D \tag{3}$$

where C and D are constants with values listed in Table 1 and T_0 is the reference absolute temperature, 295 K. The C parameter represents temperature sensitivity, which depends

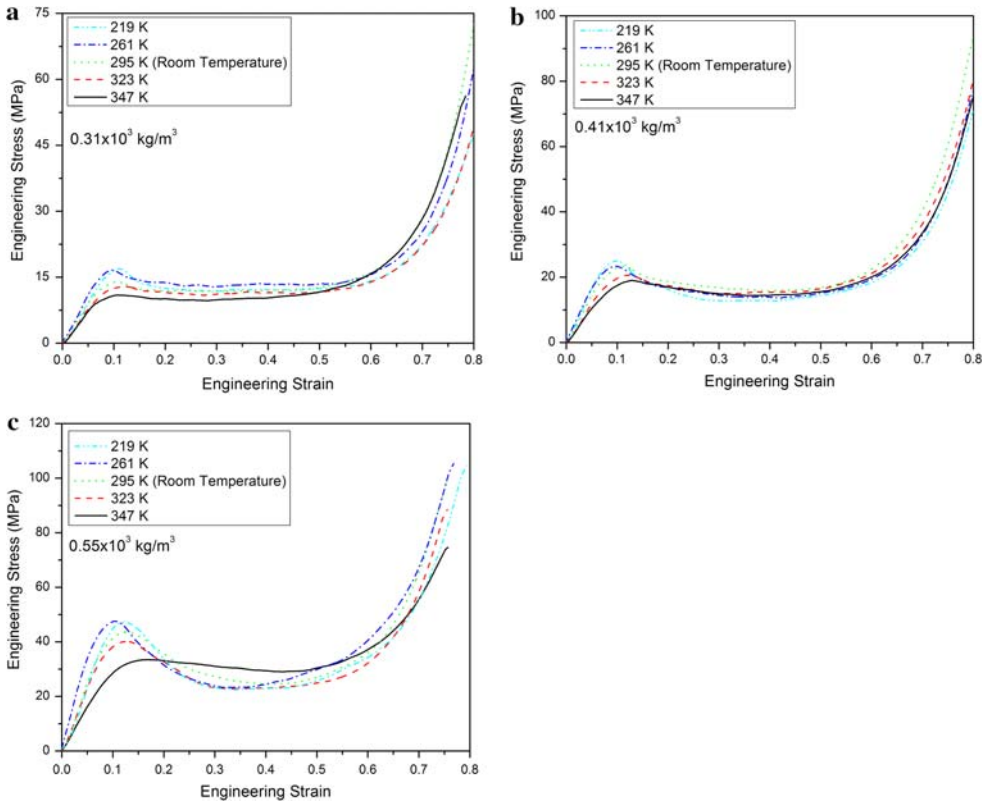

Fig. 8 Dynamic compressive stress–strain curves at 3,000 s^{-1} at various temperatures for our three foam-material densities: **a** 0.31×10^3 kg/m^3, **b** 0.41×10^3 kg/m^3, and **c** 0.55×10^3 kg/m^3

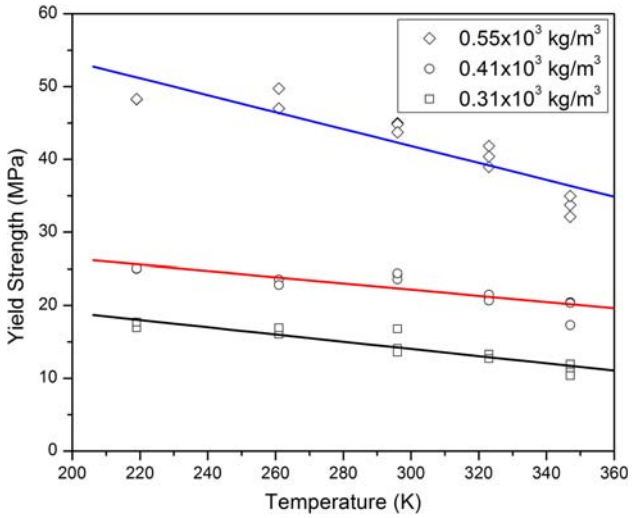

Fig. 9 Temperature sensitivities of the foam materials at different densities

on the density of the foam material. It should be noted that the above relationship of temperature sensitivity is based on the strain rate of 3×10^3 s^{-1}. This is important since temperature sensitivity may also be strain-rate dependent; that is, temperature sensitivity may be different at other strain rates (Fig. 9).

Discussion and conclusion

PMDI foam materials with three different densities were experimentally characterized by using an MTS materials testing frame, an SHPB, and an LSHPB at strain rates ranging from 10^{-2} to 10^3 s^{-1}. The yield strength of the 0.31×10^3 kg/m^3 foam in this study is very close to that obtained at the similar strain rate ($\sim 3 \times 10^3$ s^{-1}) by Bateman et al [3]. However, the yield strength at the strain rate of 640 s^{-1}, as predicted from Eq. 1, is approximately 60% higher than that obtained at the same rate by Bateman et al. This discrepancy can be attributed to Bateman et al.'s use of much longer specimens (19 and 38 mm long), which in turn decreased specimen strength.

Dynamic compressive experiments were also performed on all three foam materials at temperatures ranging from 219 to 347 K, while maintaining a fixed high strain rate of 3×10^3 s^{-1}. The effects of density, strain rate, and temperature on the compressive stress–strain response were determined. Because the deformation and damage mechanisms changed under different conditions, density, strain rate, and temperature influenced not only the yield strength but also the shape of stress–strain curves. The strain-rate and temperature sensitivities depending on material density were examined. For a certain material density, the stress–strain characteristic at high strain rates is close to that at low temperatures, whereas the stress–strain response at low strain rates is close to that at high temperatures. This is consistent to the "time–temperature" superposition principle for polymers [7, 8]. Future experiments could yield data for developing a "rate–temperature" superposition principle for PMDI foam materials.

Acknowledgements The authors would like to thank Mr. Xu Nie at Purdue University for his friendly help in obtaining scanning electron microscopy images of the foam structures. This work was performed at Purdue University and supported by Sandia National Laboratories, operated by Sandia Corporation, a Lockheed Martin Company, for the United States Department of Energy under Contract DE-AC04-94AL85000.

References

1. Gibson LJ, Ashby MF (1999) Cellular solids, structure and properties, 2nd edn. Cambridge University Press, Cambridge
2. Song B, Chen W, Frew DJ (2004) J Compos Mater 38:915
3. Bateman VI, Brown FA, Hoke DA (2001) Structural foam characteristics in a mechanical shock environment, Sandia report, SAND2001–2674
4. Song B, Chen W, Yanagita T et al (2005) Compos Struct 67:279
5. Song B, Chen W, Yanagita T et al (2005) Compos Struct 67:289
6. Song B, Chen W, Jiang X (2005) Int J Veh Des 37:185
7. Zhao J, Knauss WG, Ravichandran G (2007) Mech Time-Depend Mater 11:289
8. Williamson DM, Siviour CR, Proud WG et al (2008) J Phys D Appl Phys 41:085404
9. Jin H, Lu W-Y, Scheffel S et al (2007) Int J Solids Struct 44:6930
10. Song B, Chen W (2004) Exp Mech 44:300
11. Song B, Forrestal MJ, Chen W (2006) Exp Mech 46:127
12. Gary GT (2000) Am Soc Met 8:462
13. Zhao H, Gary G (1997) J Mech Phys Solids 45:1185
14. Song B, Syn CJ, Grupido CL et al (2008) Exp Mech. doi: 10.1007/s11340-007-9095-z
15. Song B, Chen W, Lu W-Y (2007) Int J Mech Sci 49:1336